Dependence of exchange coupling interaction on micromagnetic constants in hard/soft magnetic bilayer systems

A. J. Zambano,[1,*] H. Oguchi,[1] I. Takeuchi,[1] Y. Choi,[2,3] J. S. Jiang,[2] J. P. Liu,[3] S. E. Lofland,[4] D. Josell,[5] and L. A. Bendersky[5]
[1]*Department of Materials Science and Engineering and Center for Superconductivity Research, University of Maryland, College Park, Maryland 20742, USA*
[2]*Materials Science Division, Argonne National Laboratory, Argonne, Illinois 60439, USA*
[3]*Department of Physics, University of Texas at Arlington, Arlington, Texas 76019, USA*
[4]*Department of Physics, Rowan University, Glassboro, New Jersey 08028, USA*
[5]*National Institute of Standards and Technology, Gaithersburg, Maryland 20899, USA*
(Received 15 December 2006; published 30 April 2007)

To elucidate the dependence of exchange coupling behavior of hard/soft magnetic bilayer systems on various micromagnetic constants, the coupling length (λ) and the nucleation field (H_N) were systematically measured on five thin-film libraries made of soft magnetic/hard magnetic bilayers. Hysteresis loops of CoPt/Fe_xCo_{1-x} ($0 \leqslant x \leqslant 1$), CoPt/Ni, CoPt/Fe, Sm_2Co_7/(Fe, Co, or Ni), and Sm_2Co_7/Ni were measured using a magneto-optical Kerr effect setup. The one-dimensional model proposed by Leineweber and Kronmüller [J. Magn. Magn. Mater. **176**, 145 (1997)] and micromagnetic simulations were used to interpret the behavior of λ and H_N obtained by the high-throughput investigation. We found that the dominant factors determining λ and H_N are the hard layer magnetic constants and the saturation magnetization (M) of the soft layer. H_N and λ display a direct correlation with the domain-wall width of the hard layer and have an anticorrelation with M of the soft layers. They were found to not be substantially dependent on exchange stiffness (A) and anisotropy (K) constants within the group of soft layer materials studied here.

DOI: 10.1103/PhysRevB.75.144429 PACS number(s): 75.50.Ww, 75.30.Gw, 75.50.Vv, 75.70.−i

INTRODUCTION

Exchange coupled hard/soft magnet nanocomposites are being pursued for creating permanent magnets with substantially enhanced maximum energy products $(BH)_{max}$.[1,3–5] As a simple one-dimensional model of such magnets, bilayer thin films are frequently used to probe the exchange coupling interaction. But despite extensive effort,[2,5–8] the factors that rule the exchange coupling interaction in such bilayer systems have not been unambiguously established. There are some theoretical studies reported to date, but there is only limited experimental evidence to confirm the models. For instance, through a simple analysis, Kneller and Hawig[5] have given a rough estimate of the critical dimension of the soft layer which is ideally coupled to the hard layer and concluded that it is mainly determined by the domain-wall thickness of the hard layer. On the other hand, it has been shown that under specific limits, one can arrive at expressions for exchange field (H_{ex}) which depend only on soft layer parameters.[7,8] Other models, such as those by Skomski and Coey[9] and Leineweber and Kronmüller,[2] are more comprehensive and take into account the properties of both hard and soft layers. Because of the large number of variables involved in these ferromagnetic-bilayer systems, the ideal way to obtain an overall picture of their behavior, and compare the result to the models, is through analysis of a large number of samples where each variable is separately and continuously changed.

In this work, we report on systematically performed experiments[10] designed to delineate subtle variation of the exchange coupling behavior using a series of thin-film bilayers. We characterized the exchange coupling interaction through two quantities: the coupling length (λ) and the nucleation field (H_N), where λ is defined as the largest thickness of the soft layer that still yielded strongly coupled soft/hard layers and H_N is defined as the field at which a domain wall first nucleated in the coupled bilayer systems.[11,12] We studied the dependence of the bilayer behavior on various magnetic parameters and the thickness of the soft layer (t_s). We used the model proposed by Leineweber and Kronmüller[2] and micromagnetic simulations using a commercial solver[13] to analyze the experimental trends of λ and H_N as a function of t_s. The results of the study provided a clear picture of the roles played by exchange stiffness (A), saturation magnetization (M), and anisotropy (K) of both soft and hard layers on the exchange coupling interaction that should allow accurate prediction of the general behavior of coupled hard/soft magnetic layers.

EXPERIMENT

To systematically investigate the effect of different parameters, we used the combinatorial approach where a large number of samples are fabricated and studied simultaneously. Different combinations of hard/soft layer compositions and thicknesses consisting of CoPt(300 Å)/(Fe_xCo_{1-x}) ($0 \leqslant x \leqslant 1$), CoPt(300 Å)/Ni, CoPt(300 Å)/Fe, Sm_2Co_7(960 Å)/(Fe, Co, and Ni), and Sm_2Co_7(960 Å)/Ni were generated on five thin-film library chips. The bilayer systems were grown on 15×15 mm^2 or 7.5×15 mm^2 MgO (110) substrates by dual-gun electron-beam evaporation at a background pressure of approximately 2×10^{-6} Pa (2×10^{-8} Torr). The coercive field of the hard layer (H_c) was also systematically varied between libraries. This was achieved by changing the deposition rate or the annealing time during their growth as described below.

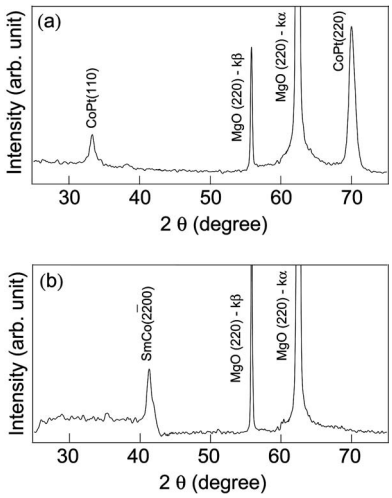

FIG. 1. X-ray diffraction (XRD) patterns of (a) CoPt and (b) nominal Sm_2Co_7. XRD using a K_α and K_β Cu source.

The (110) oriented CoPt hard magnetic layers were epitaxially grown using a Pt(10 Å) buffer layer at 600 or 700 °C. For the latter case, the hard layer was postannealed at 700 °C for 15 min. Following this, in both cases, the substrate temperature was decreased at a rate of 5 °C/min to 200 °C. The deposition rates needed to obtain the correct stoichiometry were 0.4 Å/s for Pt and 0.3 Å/s for Co. The increase in the substrate deposition temperature resulted in an increase in H_c from $\cong$0.64 to $\cong$1 T. Sm-Co films (960 Å), with the nominal composition of Sm_2Co_7 and the characteristic $(2\bar{2}00)$ orientation,[14] were grown on a Cr(200 Å) buffer layer at 450 °C The synthesis of Sm_2Co_7 by e-beam evaporation was complicated by Sm evaporation from the surface of the sample that occurred simultaneously with deposition due to Sm's high vapor pressure. To correct this, Sm was evaporated at the same rate as Co, corresponding to a slightly higher rate than that dictated by the desired stoichiometry. Deposition rates of either $\approx$2 or $\approx$4 Å/s for both Sm and Co were used, considerably higher than those used for CoPt. The two different deposition rates resulted in different values of H_c. Namely, H_c was $\approx$0.68 T for films deposited at $\approx$2 Å/s, and it was $\approx$1.32 T for those deposited at $\approx$4 Å/s. The (110) and (220) peaks of a CoPt film (300 Å) and the $(2\,\bar{2}\,00)$ peak of a Sm_2Co_7 film (1000 Å) from the x-ray diffraction shown in Figs. 1(a) and 1(b), respectively, attest to the orientations of the films.

To complete the bilayers, polycrystalline Fe and Co soft layers were deposited at 200 °C on the CoPt layer and at 100 °C on the Sm_2Co_7 layer. The different compositions of Fe_xCo_{1-x} $(0\leqslant x\leqslant 1)$ were achieved by controlling the deposition rates of the coevaporated elemental Fe and Co sources. Typical soft layer deposition rates ranged from 0.1 to 0.4 Å/s. To prevent oxidization, the samples were capped by a 75 Å thick gold layer deposited at room temperature.

In order to study the effect of changing soft phase parameters on the exchange coupling, we independently varied the composition and the thickness of the soft layer on a single square library chip using two perpendicular shadow masks.

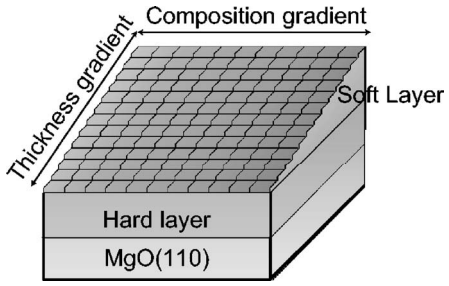

FIG. 2. Schematic of the libraries.

Along one direction, the composition of the soft phase was varied, e.g., from pure Fe to pure Co, and along the perpendicular direction, the thickness of the soft layer was changed. For the CoPt(300 Å)/(Fe_xCo_{1-x}) $(0\leqslant x\leqslant 1)$ library, the soft layer composition was varied in 11 steps and the thickness t_s was increased from 10 to 140 Å in 14 steps. In this manner, we can obtain up to 150 different combinations of soft layer composition and thickness on a single library chip. For the other libraries, only single compositions were deposited and t_s was smoothly increased from 0 to $\approx$70 Å. We now use "sample" to denote each small region of a library in which the composition and thicknesses of the soft layer are constant. A schematic of a typical bilayer library is shown in Fig. 2.

The magnetic hysteresis loops of each sample were measured using the magneto-optical Kerr effect (MOKE), which allows us to rapidly scan all the samples on a single library in one measurement session. The maximum range of the external magnetic field (H) is ±2.3 T, which is high enough to saturate our hard magnetic layers. Our MOKE laser spot size is less than 0.1 mm and the rotation angle sensitivity is $\approx 5\times 10^{-4}$ deg, which allows us to detect small changes in mag-

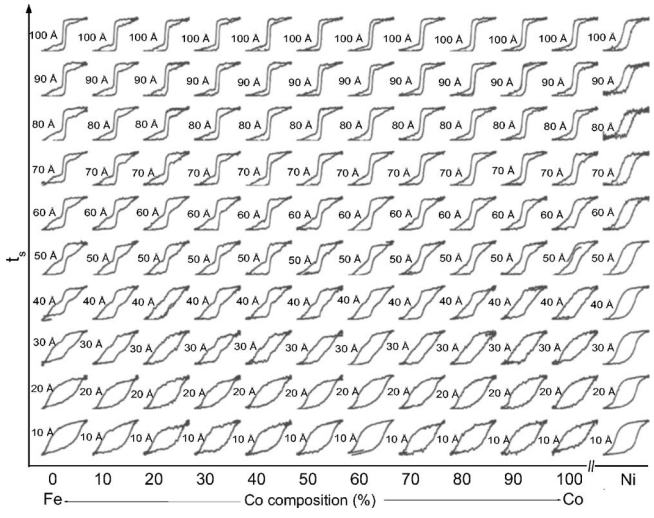

FIG. 3. Magnetic hysteresis loops (a.u.) for different soft layer thicknesses (t_s) and compositions on a CoPt($H_c\cong$0.64 T) hard layer measured on a single library. The coupling length λ_x is experimentally determined from the soft layer thickness at which the transition between one-phase-like behavior and two-phase-like behavior takes place.

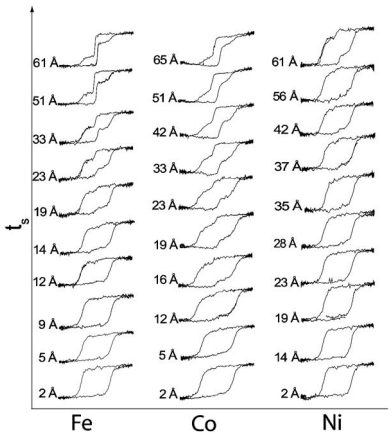

FIG. 4. Magnetic hysteresis loops (a.u.) for different soft layer thicknesses (t_s) for three elemental soft layers on a Sm_2Co_7 hard layer with coercivity $\cong 0.68$ T. The data curves are a representative subset of those obtained.

netization as we scan the laser from sample to sample on the library. By measuring the remanent magnetization vs t_s for different hard/soft layer combinations, we determined that MOKE characteristically probes a depth of ≈ 100 Å. Thus, MOKE allows us to study the magnetic properties of the bilayers very close to the interface.

RESULTS AND DISCUSSION

We tracked the hysteresis loop from each sample within the same library to ascertain its variation as a function of the soft-layer composition and thickness. An ideally exchange coupled hard/soft magnet shows a one-phase-like magnetic hysteresis loop. A partially exchange coupled magnet should exhibit a two-phase-like hysteresis loop. For each given soft layer composition, a "transition" between one-phase- and two-phase-like behaviors[5] appears as t_s increases. We define the composition-dependent thickness of the soft-layer at which the first sign of two-phase-like behavior is observed in the plots to be the coupling length (λ_x), where the subscript x denotes the soft layer composition.

Figure 3 shows hysteresis loops of Fe-Co and Ni on CoPt with $H_c \approx 0.64$ T. From such sets of loops, visual inspection along with analysis of the first derivative of the loops with respect to the applied field allow us to obtain λ_x for different soft layer compositions; the derivative of the curves shows a clear peak, where there is a drastic change in the slope in the case of the two-phase-like behavior. The fixed finite increment of the thickness variation on each library creates a lower bound to the total uncertainty of each λ_x measurement to be ±5 Å (i.e., half of the t_s increment). These uncertainties are associated with the difficulty in graphically determining the soft layer thickness at which the two-phase-like behavior first appears. The one-to-two-phase-like transition can occur as much as a full thickness step beneath λ_x. The values of λ_x reflect the trend of the transition vs soft layer composition. The uncertainty of λ_{Ni} was not assigned, due to difficulty in determining the one-to-two-phase-like transition for this soft layer composition. Because of the finite penetration depth of the laser, as t_s is increased, the MOKE signal obtains less information from the hard layer underneath the soft layer. For $t_s \geqslant 100$ Å ($\approx$MOKE laser penetration depth), all the signal comes from the soft layer, and if the soft layer is still strongly coupled to the hard layer ($\lambda_x \geqslant$MOKE laser penetration depth), the one-to-two-phase-like transition will not appear within the libraries. This was the case in the Ni magnetization loops displayed in Fig. 3, and we conclude that λ_{Ni}

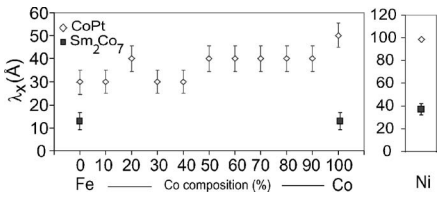

FIG. 5. Coupling length (λ_x) as a function of soft layer composition on CoPt (coercivity: $H_c \cong 0.64$ T) and Sm_2Co_7 ($H_c \cong 0.68$ T) hard layers. λ_{Ni} value is its lower limit. Composition uncertainties are not included in the graph.

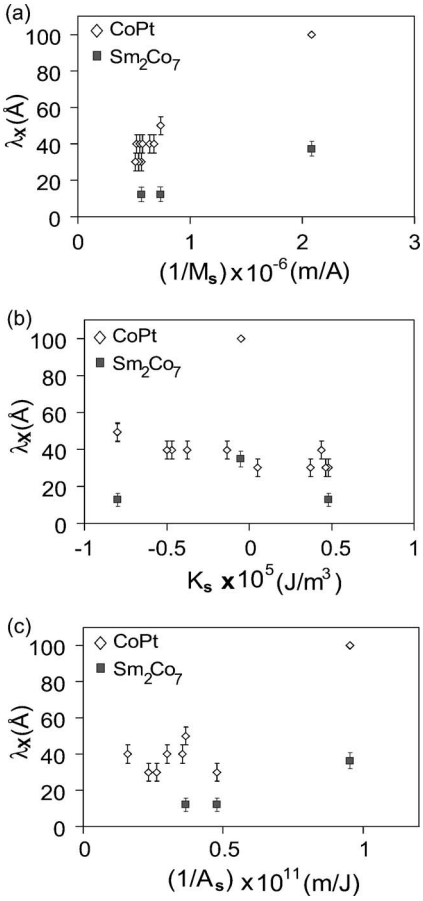

FIG. 6. Coupling length λ_x vs (a) $1/M_s$ (saturation magnetization), (b) $1/K_s$ (anisotropy constant), and (c) $1/A_s$ (exchange stiffness) of the soft layer for CoPt($H_c \cong 0.64$ T) and Sm_2Co_7 ($H_c \cong 0.68$ T) hard layers. No uncertainties were considered for the magnetic constants. Data are not shown as a function of anisotropy (A_s) for compositions $Fe_{90}Co_{10}$, $Fe_{80}Co_{20}$, $Fe_{40}Co_{60}$, and $Fe_{20}Co_{80}$ due to the absence of anistropy values for these alloys in the literature.

$\geqslant 100$ Å, however, given the data trend, we do not expect λ_{Ni} to be too much larger than 100 Å. Thus, on CoPt, while we assign λ_{Ni} to be 100 Å, it is understood to be a lower limit value. Figure 4 shows hysteresis loops of Fe, Co, and Ni on Sm_2Co_7 with $H_c \approx 0.68$ T. In this case, we consider the total uncertainty of λ_x to be approximately half of the average of the t_s increment, or ±3.5 Å.

The values of λ_x vs composition obtained from Figs. 3 and 4 are displayed in Fig. 5. The data indicate that λ_x is substantially lower for Sm_2Co_7 ($H_c \approx 0.68$ T) than for CoPt($H_c \approx 0.64$ T) even though these two hard layers have similar coercivity values; this underscores the significance of hard layer properties other than H_c in determining the exchange interaction. For CoPt($H_c \approx 0.64$ T), λ_x increases going from pure Fe to pure Co, with Ni yielding the highest value. For Sm_2Co_7 ($H_c \approx 0.68$ T), λ_x is similar for Fe and Co, but Ni has a higher value. This shows the presence of exchange coupling dependence on the soft layer elements: Ni couples more than Co to either hard layer and, in general, these two couple more than Fe.

Analysis of the variation of λ_x on the soft layer magnetic constants should reveal the mechanism involved in the soft layer coupling. However, because it is difficult to experimentally obtain the exact soft layer magnetic constants for our bilayer systems, we use typical values found in the literature, which depend on the crystalline structure. In particular, we extracted information from the Fe-Co-Ni phase diagram in Ref. 15. Ni, Co, and $Co_{90}Fe_{10}$ are face-centered cubic in structure, while the rest of the alloys are body-centered cubic. While our soft layer films are polycrystalline, because of a lack of a reliable independent technique for obtaining accurate values of these parameters for our layered structures, we used these single crystal values.[16–21] We need to keep in mind that while it is perhaps not unreasonable to expect our films to have saturation magnetization (M_s) and exchange stiffness (A_s) constants similar to those of single crystals, polycrystalline materials can have significantly lower anisotropy constant (K_s) values. We plot experimentally determined λ_x vs (a) $1/M_s$, (b) K_s, and (c) $1/A_s$ in Fig. 6. Although the effects of these parameters are expected to be correlated, separate trends can still be revealed.[2,7,8] In particular, there appears to be a linear correlation between λ_x vs $1/M_s$, while the correlations are less clear for λ_x vs K_s and λ_x vs $1/A_s$. This seems to indicate that within the layered systems studied here, for which $K_h/K_s > 100$ with K_h being the hard layer anisotropy constant, M_s has the largest influence on λ_x. On the other hand, it has previously been noted that the exchange coupling is strongly affected by K_s if the anisotropy of the hard and soft layers are such that $K_h/K_s \approx 10$.[8]

We also observed a dependence of λ_x on the hard layer coercivity. Figure 7(a) shows the hysteresis loops of Fe/CoPt samples for two different coercivity values of CoPt. From these loops, we determined that $\lambda_{Fe} \approx 30$ Å and $\lambda_{Fe} \approx 20$ Å for $H_c \approx 0.64$ T and $H_c \approx 1$ T, respectively. This represents a reduction of ≈30% in λ_{Fe} for ≈56% increase in H_c. Similarly, Fig. 7(b) shows the hysteresis loops of Ni/Sm_2Co_7 for two different coercivities of Sm_2Co_7. From these loops, we determined that $\lambda_{Ni} \approx 37$ Å and $\lambda_{Ni} \approx 15$ Å for $H_c \approx 0.68$ T and $H_c \approx 1.32$ T, respectively. This represents a reduction of ≈60% in λ_{Ni} for ≈100% increase in H_c. If the other hard layer properties did, in fact, not change, these results would indicate that increasing the hard-layer coercive field decreases the coupling length.

The rotation behavior of the magnetization at the soft/hard interface determines the characteristics of the hysteresis loops. Specifically, whether the rotation of the polarization as a function of H and as a function of the position within the film, as depicted in Fig. 8, is gradual or abrupt determines the nature of the transition from one- to two-phase-like magnetization loops. In carefully comparing loops in Figs. 3, 4, 7(a), and 7(b), the samples in CoPt libraries display a smoother transition between one- and two-phase-like behaviors than those in Sm_2Co_7 libraries. This transition is a measure of the strength of the soft/hard-layer interaction. Namely, smoother transitions indicate wider domain walls, which, in turn, are associated with the compliance of the hard layer to the influence of the soft layer. The observed trend indicates that the influence of the soft layer on the hard layer is weaker in the Sm_2Co_7 samples than in the CoPt. As discussed below, this can be explained in terms of the domain walls within the hard layer.

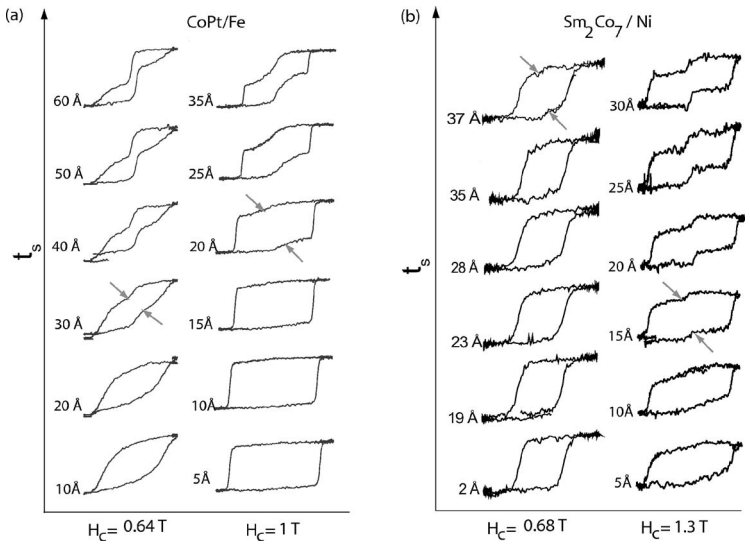

FIG. 7. Magnetic hysteresis loops (a.u.) for a range of soft layer thicknesses t_s on (a) CoPt and (b) Sm_2Co_7 hard layers possessing two different coercivities (H_c). The arrows indicate the locations on the hysteresis loops where two-phase-like behavior is first observed with increasing t_s.

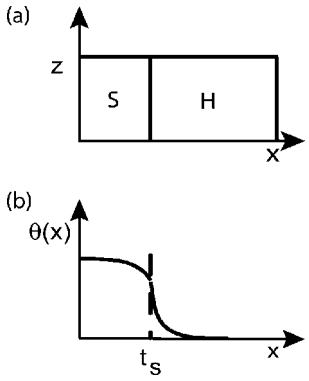

FIG. 8. Schematic of the system used in the model by Leineweber and co-workers (Refs. 2 and 22). (a) Soft layer (S)/ hard layer (H) system. The position x is taken from the top of the soft layer surface, with z the direction in the film plane that is parallel to the external field. (b) The in-plane angle θ defining the polarization of the magnetization as a function of x, where t_s, the soft layer thickness, marks the location of the soft/hard layer interface.

In Figs. 3 and 4, one can clearly discern a continuous shape change of the hysteresis loops together with a change of the coercivity along the y axis. We graphically determine the nucleation field H_N for each hysteresis loop, i.e., the field at which the slope of the curve during the demagnetization process starts to change substantially. This value is equated to the value of H, where the tangent to the loop at the point with maximum magnetization intercepts the tangent to the loop at the point of maximum slope (see Fig. 9 inset, points marked "A"). As seen in Figs. 3 and 4, the nucleation field thus determined shifts substantially when the behavior transitions from one-phase-like to two-phase-like in addition to significant systematic variation across the full range of t_s values.

Figure 9 displays the experimental values of H_N vs t_s, for Fe, Co, and Ni on Sm_2Co_7 ($H_c \approx 0.68$ T) and CoPt($H_c \approx 0.64$ T). The data follow the same general trend, with H_N decreasing from approximately H_c toward an asymptotic minimum value as t_s increases from 0. The thickness range where H_N decreases most rapidly corresponds to the appearance of the two-phase-like behavior in the magnetization loops. One might expect that the nucleation field decreases most rapidly when the soft layer thickness t_s approximately equals the coupling length λ_x. The behavior depends on both the hard layer and the soft layer. Broadly speaking, the nucleation fields are higher with the CoPt hard layer than the Sm_7Co_2 for a given thickness of soft Fe, Ni, or Co (the exception being thin Ni). Also, the nucleation field H_N decreases more smoothly with thickening of the Co and Ni soft layers for the CoPt hard layer versus the Sm_7Co_2. The results, along with the behavior observed for λ_x, indicate that soft layers with lower saturation magnetization are exchange coupled more to the given hard layer, while the exchange coupling interaction is impacted by the hard layer characteristics as one might expect.

To obtain more insight about the effect of the micromagnetic constants on the exchange coupling, we utilized the model of Leineweber and Kronmüller.[2] This model gives the irreversibility field (H_{irr}), which ideally corresponds to the

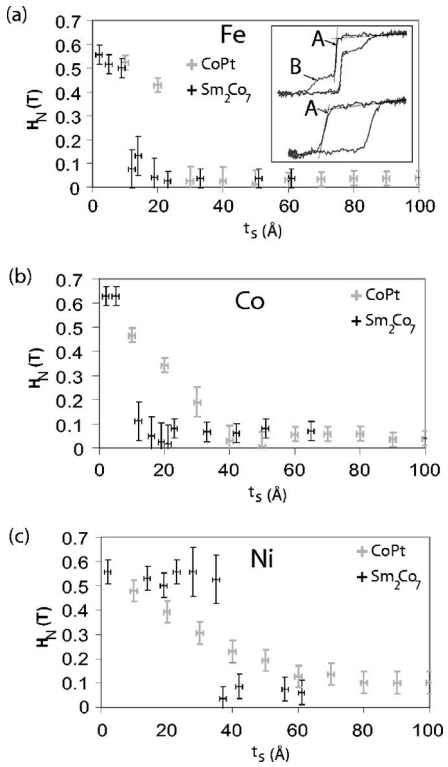

FIG. 9. The nucleation field (H_N) as a function of the soft layer thickness t_s for soft layers (a) Fe, (b) Co, and (c) Ni. The symbols are experimental data. Results are shown for both Sm_2Co_7 ($H_c \cong 0.68$ T) and CoPt($H_c \cong 0.64$ T) hard layers. The indicated uncertainties in H_N were graphically determined. Inset: graphical determination of H_N, marked A, and the ideal irreversible field H_{irr}, marked B.

field at point B in the inset of Fig. 9(a), as a function of t_s. From H_{irr} vs t_s for the different material systems, we can obtain the dependence of the coupling length λ_x on the magnetic constants. To find the general trend in the H_{irr} vs t_s curve with independently changed magnetic constants, we analyzed a particular Fe/SmCo bilayer (Fig. 10). Figure 8 shows a schematic of the system. In the model, the Gibb's energy of the system is minimized and the resulting Euler-Lagrange equations are solved to obtain the rotation of the in-plane polarization $\theta(x,H,t_s)$ as a function of the position x. Using the model and following the same stability analysis technique described in Refs. 2 and 22, H_{irr} vs t_s was numerically calculated for t_s over the full range from 100 to 0 Å. Below the thickness $t_s = t_o$, H_{irr} was considered to be equal to the ideal irreversible field of the hard layer.[2,20] The model assumes that for $t < t_o$, the coupling between the hard/soft layers is maximized, which in an ideal case represents complete coupling. Thus, t_o is equivalent to our experimentally obtained λ_x values. The magnetic constants used for these calculations are shown in the caption of Fig. 10. The overall trends predicted by the model for variation of the properties of the soft magnetic material are as follows: λ_x increases with decreasing M_s, while it is barely affected by changes in A_s and not affected by changes in K_s in the range of values used, which roughly correspond to those of the soft material studied here. For variation of the hard magnetic material

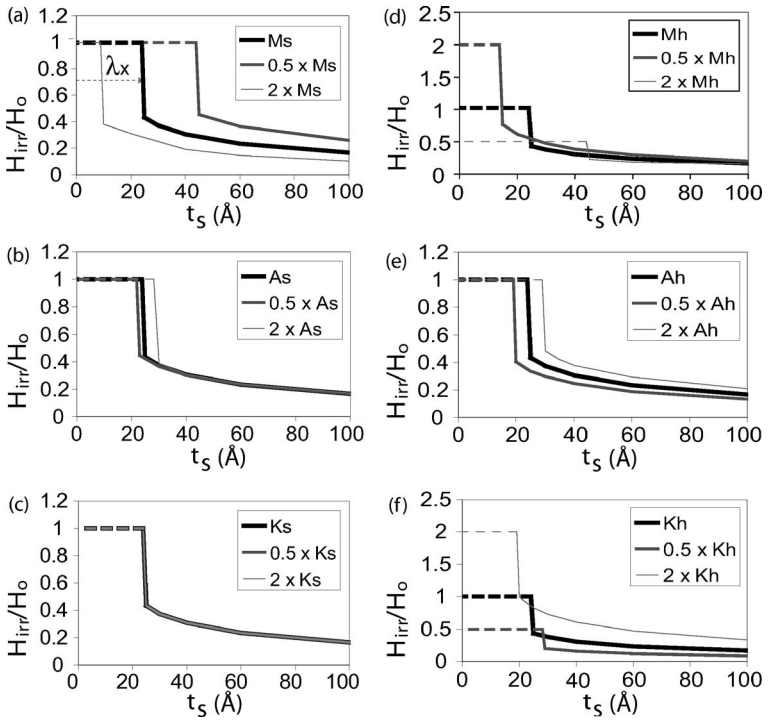

FIG. 10. Numerical calculations of the irreversible field (H_{irr}) of SmCo/Fe(t_s) as functions of the soft layer thickness t_s obtained from the model by Leineweber and co-workers (Refs. 2 and 22). λ_x is the coupling length and $H_o = 2K_h/M_h$. Magnetic constants used are $K_s \cong 0.48\times10^5$ J/m^3, $M_s \cong 1.7\times10^6$ A/m, $A_s \cong 2.7\times10^{-11}$ J/m, $K_h \cong 5\times10^6$ J/m^3, $M_h \cong 5.5\times10^5$ A/m, and $A_h \cong 1.2\times10^{-11}$ J/m.

properties, it is found that λ_x increases as M_h or A_h increases and decreases as K_h increases.

For comparison, we also modeled the spin configurations in SmCo(200 Å)/Fe(60 Å) bilayers using the LLG Micromagnetics Simulator®.[3] In these simulations, not shown, each bilayer is approximated as a stack of 52 three-dimensional-cells spanning the thickness of the film as well as covering its full area; the magnetic configuration uniform within each cell was uniform and independently variable from that in other cells. The magnetic constants used to find the equilibrium configurations in the simulations are the same as those used to obtain the results shown in Fig. 10. The general trends in H_{irr} shown by the two calculations are in good agreement. For instance, when K_h is increased, H_{irr} (t_s=60 Å) is increased; when K_s is changed in the present range of $K_h/K_s > 100$, H_{irr} is nearly unaffected.

The dependence of λ_x, obtained from the model of Leineweber and co-workers,[2,22] on independently changed soft layer magnetic constants agrees with the experimental observations. This indicates that the soft materials that most effectively increase the coupling length are those with lower M_s.

The experimental results when the hard layer is changed are also interpreted using the calculation results. The magnetic constants of bulk hard materials [CoPt and Sm_2Co_7] are such that $K_{CoPt} \leqslant K_{SmCo}$, $M_{CoPt} \geqslant M_{SmCo}$, and $A_{CoPt} \geqslant A_{SmCo}$. If the magnetic characteristics of the thin-film hard layers are similar to those of bulk materials, the model by Leineweber and Kronmüller[2] indicates that $\lambda_{x-CoPt} \geqslant \lambda_{x-SmCo}$ would be expected for a hard-soft stack with generally soft material x. This is consistent with what is experimentally observed. Specifically, for M_h and A_h unchanged, higher H_c corresponds to higher K_h and thus prediction of a reduced λ_x in agreement with the decrease of the experimental λ_x with increasing coercivity observed experimentally in Fig. 7.

The model by Leineweber and co-workers[2,22] takes into account both the hard and soft layer properties. The spatial variation of the magnetization through the bilayer, $\theta(x,H,t_s)$, depends on the domain-wall width of both the soft layer and the hard layer, which we denote as DW_s and DW_h, respectively. The solution of $\theta(x,H,t_s)$ indicates that for a given set of magnetic constants of the soft layer, magnetic field H and soft layer thickness t_s, hard materials with a larger $DW_h = \pi\sqrt{A_h/K_h}$ induce a more gradual change in the rotation of the polarization as a function of the position within the bilayer film (particularly at the interface). Based on values given in the literature, $DW_{CoPt} \approx 100$ Å,[17] which is longer than $DW_{SmCo} \approx 50$ Å,[3] the typical domain-wall width of Sm_2Co_7. Thus, we expect CoPt-based samples to have a more gradual change in the rotation of the polarization at the interface than Sm_2Co_7-based samples. This prediction is consistent with the experimental observations, which show an inverse correlation between λ_x and DW_h (as discussed above, CoPt has longer λ_x than Sm_2Co_7). Thus, the larger the DW_h of the hard material, the stronger the interaction with the soft phase.

Based on these empirical results, we consider a simple linear relation between M_s and λ_x, namely, $\lambda_x = -M_s\alpha + \beta$, where α and β are positive constants. This allows us to determine the volume fraction of the soft layer which contributes to the saturation magnetization in an ideally coupled system (volume=sample area$\times\lambda$). A simple calculation of the maximum energy product, assuming square magnetization loops and considering the contribution of both hard and soft magnetic layers to the saturation magnetization, indicates that $(BH)_{max}$ can be maximized by reducing the thickness of the hard layer down to $\approx DW_h$ and by increasing the thickness of the soft layer up to $\approx\lambda_x$. However, because of the inverse relation between M_s and λ_x, the soft material with the longest λ_x is not necessarily the most effective material for maximizing $(BH)_{max}$. For instance, assuming $M_h = 5.5\times10^5$ A/m, we calculate that for $DW_h \approx 50$ Å (typical value

of Sm_2Co_7), $(BH)_{max}$ can be as high as ≈21 MG Oe if a soft layer with $M_s \approx 1.3 \times 10^6$ A/m is used; and for a DW_h ≈100 Å (typical value of CoPt), $(BH)_{max}$ can be as high as ≈28 MG Oe if a soft layer with $M_s \approx 1.6 \times 10^6$ A/m is used. Therefore, changing the hard layer from CoPt to Sm_2Co_7[7] which has slightly higher coercivity, does not necessarily lead to an enhancement of the energy product.

CONCLUSIONS

In conclusion, the high-throughput hard/soft magnetic layer experiments show a trend indicating that the hard layer magnetic parameters and the saturation magnetization of the soft layer play the most important roles in determining the nucleation field and the coupling length. Hard materials with higher coercivity do not necessarily benefit the soft/hard phase interaction. There is an inverse relation between the width of the domain wall of the hard layer and the exchange coupling interaction. In the range of exchange stiffness K_s and anisotropy constant A_s values used in this experiments, the saturation magnetization M_s is the principal parameter of the soft layer that governs the exchange interaction: the higher the M_s, the stronger the exchange interaction. A trade-off between coercivity and exchange interaction is observed: hard phases with higher coercivity do not necessarily result in an enhancement of energy product. Similarly, because of the trade-off between saturation magnetization and exchange length, soft materials with the longer coupling length do not always result in an enhancement of the energy product.

ACKNOWLEDGMENTS

This work was supported by ONR/MURI under Grant No. N00014-05-1-0497 and by NSF Grant No. DMR 0231291. Work at Argonne was supported by U.S. DOE Office of Science under Contract No. DE-AC02-06CH11357.

*Corresponding author. Electronic address: azambano@umd.edu

[1] R. Andreescu and M. J. O'Shera, J. Appl. Phys. **97**, 10F302 (2005), and references therein.
[2] T. Leineweber and H. Kronmüller, J. Magn. Magn. Mater. **176**, 145 (1997).
[3] Eric E. Fullerton, J. S. Jiang, and S. D. Bader, J. Magn. Magn. Mater. **200**, 392 (1999).
[4] J. Zhou, R. Skomski, Y. Liu, Y. C. Sui, W. Liu, and D. J. Sellmyer, J. Appl. Phys. **97**, 10K304 (2005).
[5] E. F. Kneller and R. Hawig, IEEE Trans. Magn. **27**, 3588 (1991).
[6] J. S. Jiang, J. E. Pearson, Z. Y. Liu, B. Kabius, S. Trasobares, D. J. Miller, S. D. Bader, D. R. Lee, D. Haskel, G. Srajer, and J. P. Liu, J. Appl. Phys. **97**, 10K311 (2005), and references therein.
[7] E. Goto, N. Hayashi, T. Miyashita, and Keisuke Nakagawa, J. Appl. Phys. **36**, 2951 (1965).
[8] Z. J. Guo, J. S. Jiang, J. E. Pearson, S. D. Bader, and J. P. Liu, Appl. Phys. Lett. **81**, 2029 (2002).
[9] Ralph Skomski and J. M. D. Coey, Phys. Rev. B **48**, 15812 (1993).
[10] I. Takeuchi, O. O. Famodu, J. C. Read, M. A. Aronova, K.-S. Chang, C. Craciunescu, S. E. Lofland, M. Wuttig, F. C. Wellstood, L. Knauss, and A. Orozco, Nat. Mater. **2**, 180 (2003).
[11] O. Hellwig, J. B. Kortright, K. Takano, and Eric E. Fullerton, Phys. Rev. B **62**, 11694 (2000).
[12] Eric E. Fullerton, J. S. Jiang, M. Grimsditch, C. H. Sowers, and S. D. Bader, Phys. Rev. B **58**, 12193 (1998).
[13] Commercial micromagnetics solver by Michael Scheinfein (http://llgmicro.home.mindspring.com). Corporate and product names are included only for completeness of description. They do not constitute endorsement by NIST.
[14] Eric E. Fullerton, J. S. Jiang, Christine Rehm, C. H. Sowers, S. D. Bader, J. B. Patel, and X. Z. Wu, Appl. Phys. Lett. **71**, 1579 (2005).
[15] Y. K. Yoo, Q. Xue, Y. S. Chu, S. Xu, U. Hangen, H. Lee, W. Stein, and X. Xiang, Intermetallics **14**, 241 (2006).
[16] R. S. Sundar and S. C. Deevi, Int. Mater. Rev. **50**, 157 (2005).
[17] K. H. J. Buschow, *Magnetism and Processing of Permanent Magnet Materials* (North Holland, Amsterdam, 1997), Vol. 10, Table 12.1, p. 575.
[18] O. Petracic, Z.-P. Li, I. V. Roschchin, M. Viret, R. Morales, X. Batlle, and I. K. Shuller, Appl. Phys. Lett. **87**, 222509 (2005).
[19] X. Liu, R. Sooryakumar, C. J. Gutierrez, and G. A. Prinz, J. Appl. Phys. **75**, 7021 (1994).
[20] M. R. Pufall, W. H. Rippard, and T. J. Silva, Appl. Phys. Lett. **83**, 323 (2003).
[21] I. Turek, J. Kudrnovsky, V. Drchal, P. Bruno, and S. Blügel, Phys. Status Solidi B **236**, 318 (2003).
[22] R. Fischer, T. Leineweber, and H. Kronmüller, Phys. Rev. B **57**, 10723 (1998).